

Electrodeposition of CoNiMnP Thick Films for Micromachined Magnetic Device Applications

PAULA BARBU, MIRELA MARIA CODESCU*, MIHAI IORDOC, VIRGIL MARINESCU, EUGEN MANTA, CRISTINEL ILIE, MARIUS POPA

R&D National Institute for Electrical Engineering ICPE-CA Bucharest, 313 Splaiul Unirii, 030138, Bucharest, Romania

CoNiMnP permanent magnetic alloys were electrodeposited on copper and brass substrates from a bath containing 26 g/L $\text{CoCl}_2 \cdot 6\text{H}_2\text{O}$, 24 g/L $\text{NiCl}_2 \cdot 6\text{H}_2\text{O}$, 3.6 g/L MnSO_4 , 4.6 g/L $\text{NaH}_2\text{PO}_4 \cdot \text{H}_2\text{O}$ as precursors and H_3BO_3 , NaCl, saccharin, sodium lauryl sulphate and cerium(III) sulphate as additives. Influence of the presence of external magnetic field (2 T) was investigated using vibrating sample magnetometry and SEM/EDS microscopy.

Keywords: CoNiMnP alloys, magnetic MEMS, thick film electrodeposition, magnetometry, microscopy characterization

Devices based on the micro-electro-mechanical systems (MEMS) include components for different applications: microactuators, microsensors, micromotors, micropumps, microvalves, microswitches, etc [1, 2]. New and efficient MEMS devices can incorporate permanent magnetic materials [3 - 5]. Magnetic components can generate higher forces at a larger distance than their electrostatic counterparts; the energy density between the magnetic plates is usually longer than that between the electric plates [6]. Typical examples of magnetic actuators among other above mentioned are optical switches and attenuators, micro-relays and magnetic energy harvesters. Magnetic sensors applications include thin film recording read-write heads, magneto-resistive devices and magnetic field sensors. Magnetic material may be *soft* (magnetization direction is easily changed), *hard* (magnetization direction is difficult to change) or magnetostrictive material. The soft magnetic materials may be NiFe or CoFe, CoPt, PtMn or IrMn thin films.

The hard magnetic materials have a number of advantages over soft ones, including higher magnetic energy density, and the corresponding devices may utilize thicker layers. The hard magnetic films can be prepared by different techniques: magnetron sputtering [7, 8], PLD [9, 10], CVD [11], electroless [12], electrodeposition [13]. Recently there has been a growing interest in the realization of MEMS devices with hard magnetic films having benefits from constant energy stored in magnet, low power consumption, favorable scaling and simple electronic circuit [14 - 16]. However, their fabrication in the micro scale is limited mainly by technical difficulties in obtaining precise thickness (in general more than 10 nm, since magnetic force depends on material volume).

The most facile method for integrate the magnetic components, but with constraints concerning the minimal sizes of the permanent magnets, was the production of bonded magnets, starting from microcrystalline based rare-earths powders [17].

Electrodeposition is the most promising and efficient preparation technique already used by us in MEMS processing [18]. This procedure is recommended for its simple setup, precisely controlled operation, capability to handle complex geometries, low cost and potential compatibility with miniaturization and high performance packaging. The prepared magnetic thin films must have good adhesion, low-stress, high corrosion resistance, and

can be thermally stable with excellent magnetic properties. The properties of materials can be 'tailored' by controlling the solution composition and the deposition parameters. To date, many researches were focused on electrodeposition of magnetic films of alloys for MEMS such as permalloy ($\text{Ni}_{80}\text{Fe}_{20}$) [19 - 21] CoNi and FeCoNi [22 - 30], CoP and CoNiP [28, 31 - 34], CoPt and CoPtP [35], and CoMnP [36].

There has been an increasing effort for the development of the permanent magnets in an integrated thick films having a higher coercivity (H_c) and maximum magnetic energy density ($(\text{BH})_{\text{max}}$). Ahn and his group [37 - 39] have successfully electrodeposited CoNiMnP alloys and their composites as microarray configurations in an external magnetic field. A CoNiMnP array consisted in permanent magnets with 10 kJ/m^3 energy density was first fabricated [37]. Using EDS elemental analysis, the authors established that the magnet arrays composition is: 84 - 85% Co, 7 - 9% Ni, 0.5 - 1.3 % Mn and 5 - 7 % P in atomic percentage scale. Co content in the film, which is responsible for high coercivity, was kept at these high values by controlling the bath composition. In another work [39] these authors have electroplated CoNiMnP arrays which were integrated into a MEMS-based silicon cantilever beam magnetic actuator; the following performances of electromagnets in the arrays were obtained: $H_c = (0.56 - 0.88) \cdot 10^5 \text{ A/m}$, residual induction $B_r = 0.17 - 0.19 \text{ T}$, $(\text{BH})_{\text{max}} = 1.9 - 2.3 \text{ kJ/m}^3$.

A comprehensive investigation of the relationship between the residual stress and the various processing parameters is needed. It is also important to develop new residual stress relievers to reduce the film stress and to eliminate the microcracks. Guan and Nelson [40] reported the electrodeposition of this kind of CoNiMnP hard magnetic film with a low residual stress, useful for MEMS applications. Sodium saccharine and a rare-earth salts mixture of $\text{Ce}_2(\text{SO}_4)_3$ and $\text{Nd}_2(\text{SO}_4)_3$ were dissolved in the bath for reducing residual stress and to improve the surface morphology. Additionally, the electrolysis parameters including applied current density, film thickness, electrolyte agitation, electrolyte pH, and temperature were optimized to provide thick films with low residual stress. A description of optimization (using Taguchi design of experiments) of both electrodeposition bath and electrolysis procedure for obtaining a $4 \mu\text{m}$ thick electroplated CoNiMnP alloy was reported by Grapes and Morris [41, 42]; from their work, a new process recipe resulted which yielded a maximum energy density of 5.3 kJ/m^3 , a remanence of 220 mT and a

* email: mirela.codescu@icpe-ca.ro

coercivity of $0.93 \cdot 10^5$ A^m. Sun, Yuan, Fang and Zhang [43, 44] described the fabrication of an electroplated CoNiMnP permanent magnet arrays, containing cylinder magnets with various radius as well as cubic magnets with different aspect ratio; this system can be utilized for novel electromagnetic energy harvester.

Qu and Jiao [45, 46] reported the fabrication of the CoNiMnP-BaFe₁₂O₁₉ nanocomposites which have been electrodeposited from an aqueous bath containing BaFe₁₂O₁₉ nanoparticles. The maximum nanoparticles fraction of ~21.8 wt. % BaFe₁₂O₁₉ was successfully embedded [45]. The authors noticed a strong influence of ferromagnetic nanoparticles concentration in the bath on the amount of incorporated nanoparticles in CoNiMnP matrix, as well as the changes in surface morphology, preferred orientation, coercivity, retentivity, and the maximum energy density. A main observation shows that the incorporation of BaFe₁₂O₁₉ nanoparticles favors the electrodeposition of Co and Mn metals, such depressing the deposition of Ni and P components, but also may change the grain size and preferred orientation within the nanocomposite structure. Also, the addition of sodium lauryl sulphate in the concentration range from 0.8 to 4 g L⁻¹ has favored the inclusion of magnetic particles into alloy deposit [46]. Thus, CoNiMnP-BaFe₁₂O₁₉ nanocomposite films with a coercivity of 1438 Oe (114 kA/m), retentivity of 0.39 T and maximum magnetic energy density of $15.41 \cdot 10^3$ kJ/ m³ has been obtained for a 3 g/L sodium lauryl sulphate concentration in the bath.

This paper presents experiments of obtaining CoNiMnP permanent magnetic alloys electrodeposited on copper and brass substrates in order to optimize the electrolysis conditions and to obtain suitable properties of the magnetic films for numerous MEMS applications. Benefited from low temperature batch fabrication the CoNiMnP thick films can be easily produced at low cost on the substrate, while eliminating alignment inaccuracy and controlling precise dimension in the micro scale. The work is a continuation of previously published paper [47] about preparation of cobalt nickel manganese-phosphorus film by electrolysis in an external magnetic field.

Experimental part

The electrolytic bath used for CoNiMnP electrodeposition has contained 26 g/L CoCl₂·6H₂O, 24 g/L NiCl₂·6H₂O, 3.6 g/L MnSO₄, 4.6 g/L NaH₂PO₄·H₂O, 24 g/L H₃BO₃, 23 g/L NaCl, 0.8 g/L saccharin, 0.1 g/L sodium lauryl sulphate and 0.01 g/L cerium(III) sulphate. All reagents were purchased from Sigma Aldrich. A value of pH=2.8 of the electrolyte was maintained using an Inolab pH meter. It is worth mentioning that for the total concentration of Co and Ni metal ions is recommended to be 0.2 M in equal proportion, respectively [CoCl₂] = [NiCl₂] = 0.1 M, and this bath used complies with this conditions.

The substrate materials, as rectangular Cu or brass plates, were cut to different sizes. Prior to electroplating, the substrate surface was polished gradually with 800-2000 grit silicon carbide paper and treated at 25-30°C in the following sequences: degreasing for 2 min. with acetone (or ethylic alcohol), rinsing successively with HNO₃ (1 : 1) aqueous solution (chemical deoxidation for 0.5 - 1 min.), running water and distilled water, and finally drying in air. The electrodeposition was carried out at room temperature in galvanostatic conditions using maximum 2 mA/cm² current density delivered by a dc power supply of 1 A and 30 V. A thickness of ca. 100 μm was expected to be achieved for an electrolysis time of 24 h. The electrolysis cell contained the substrate plate (Cu, brass) as cathode

and a Ni plate and a Co plate as soluble anodes, both with large surface area. The cell was surrounded with permanent magnets, assuring the external magnetic field $H_{ext} = 2$ T.

The electrolyte was stirred moderately using a Heidolph mechanical overhead stirrer which rotates with a common rotation rate (40 - 44 rpm). After electrolysis, the cathode was removed from the cell and the NiCoMnP deposit was washed well with water and dried.

There were 5 types of investigated samples from which 2 were of macroscopic size (32 and 17 cm²) and 3 were on microscale size (24 mm²). In order to perform electrodeposition on micro sized samples five identical pieces were connected in a comb structure (fig. 1).



Fig. 1. The arrangement of 5 identical pieces in the electrolysis vessel (a) and their connection in a comb structure (b)

The thickness of coating (d) was determined gravimetrically and calculated with using eq. (1):

$$\delta = \frac{m_p}{S \cdot \rho} \quad (1)$$

where: m_p - the weighed mass of deposit, S - the measured surface area of sample, ρ - the alloy density (calculated using $\rho_{Ni} = 8.9$ g/cm³ and $\rho_{Co} = 8.9$ g/cm³ and percentages). The electrodeposition efficiency η was calculated as ratio between the weighed deposited mass and theoretically deposited mass, according Faraday's law, using $n = 2$ for the transferred electrons.

Scanning electron micrographs (SEM) of NiCoMnP alloy films were recorded using FESEM-FIB Auriga Model microscope (Carl Zeiss) provided with secondary electron detector. The elemental analysis of coatings was performed with an EDS (energy dispersive X-ray spectroscopy) device type IncaPET X3 from Oxford Instruments. The magnetic measurements were performed by vibrating sample magnetometry (Lake Shore type magnetometer), and the main magnetic characteristics of CoNiMnP alloy films were extracted from the $M = M(H)$ plotted hysteresis curves.

Results and discussions

Five types of coatings have been experimented, that are described in Table 1 together with the bath characteristics and electrolysis conditions, including the placement in magnetic field. Temperature was always maintained constant at 25°C (room temperature). Values of 90 -92% for the current efficiency were determined proving a good selection of bath and electrodeposition condition. The last column in table 1 presents the thickness and general appearance of sample coatings.

Characterization of type 1 CoNiMnP alloys coatings (deposited on brass, external magnetic field)

Figures 2 show some SEM micrographs recorded for CoNiMnP coatings deposited onto macrosized brass substrate (32 cm²). The deposits were smooth, bright and have a light gray color. However, as figures 2a, b show, some

Table 1
TYPES OF COATINGS, ELECTROLYSIS CONDITIONS AND COATING CHARACTERIZATION

Sample type	Substrate nature	Surface area, cm ²	Bath pH	Stirring of bath	Presence of magnetic field	Current density, mA/cm ²	Electrolysis time, hours	Thickness, μm , and appearance of coating
1	brass	32	2.8	yes	no	2	24	100 (adherent, bright, uniform)
2	Cu	17	2.8	yes	yes	2	24	100 (glossy, exfoliating)
3 (5 identical pieces)	brass	24	2.8	yes	yes	0.9	32	< 0.1 (could not be magnetically measured)
4 (5 identical pieces)	brass	24	2.8	yes	yes	2.1	72	500 (non-adherent deposition with dendrite on the edges and agglomerations of material)
5 (5 identical pieces)	brass	24	2.8	yes	yes	2	24	200 (adherent, glossy, uniform over the entire surface)

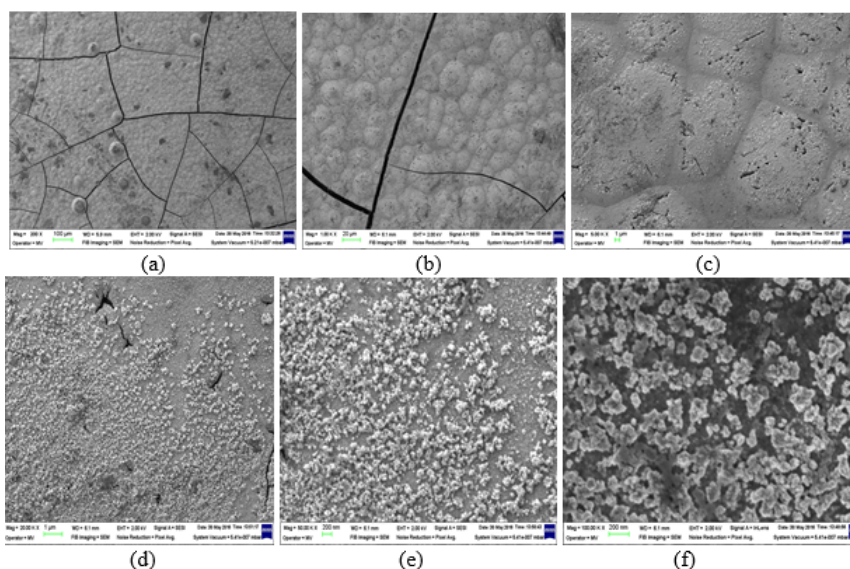


Fig. 2. Surface morphology of another type 1 CoNiMnP coating investigated by SEM at different magnifications: $\times 200$ (a), $\times 1000$ (b), $\times 5000$ (c), $\times 20000$ (d), $\times 50000$ (e), and $\times 100000$ (f)

microcracks are present on the surface of coatings that prove the presence of stress forces inside the grown deposit; this observation may be correlated with both insufficient concentration of sodium lauryl sulphate or the

absence of external magnetic field during electro-deposition.

Figures 3a - f represent the results of elemental analysis obtained by EDS spectroscopy in 6 points of the two

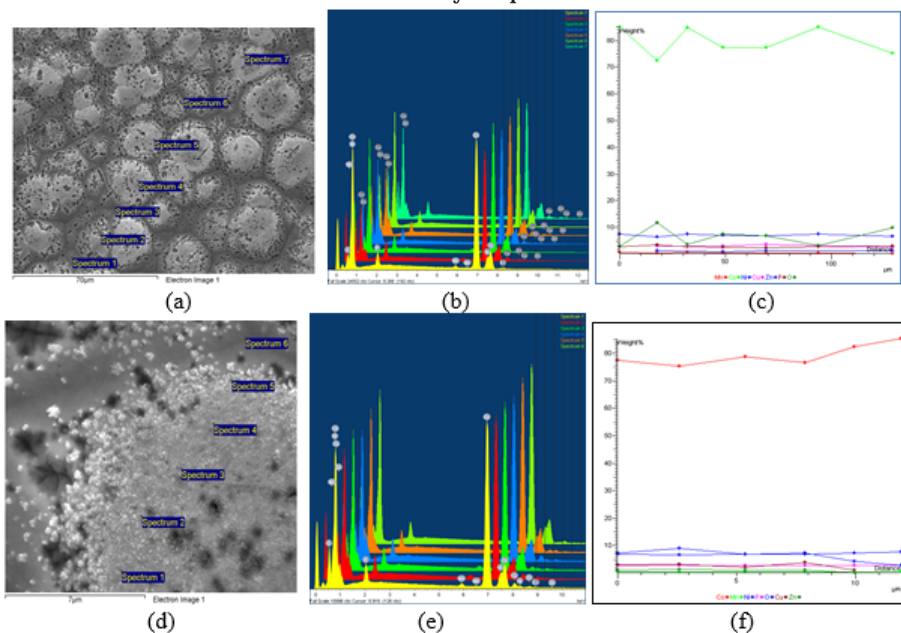


Fig. 3. Secondary electron images (a, d) for a CoMnNiP alloy electrodeposited in the absence of external magnetic field. EDS spectra (b, e) were determined in the two selected areas: microarea 1 (a-c) and microarea 2 (d-f). Distributions of concentration for each element with distance between points (relative distributions) are shown in (c) and (f), respectively

selected microareas of the same CoMnNiP sample. Both secondary electron images show an insular-type morphology containing fine spherical nodules that are evenly spread, whose composition is rich in cobalt according to distributions (c) and (f) in figure 3. For the microarea 1, the coating composition was: 72 - 85 wt.% Co, 6.5 - 7.7 wt.% Ni, 0.5 - 0.8 wt.% Mn and 2.6 - 3.7 wt.% P. For microarea 2 of the same sample it is found that the deposited alloy also has a high content of cobalt (75 - 85 wt.% Co), whereas the nickel content is between 6.70 and 7.90 wt.%, the manganese content is between 0.60 and 0.74 wt.% and the phosphorus is 2.9 - 3.0 wt.%. The distributions of the concentration of the highlighted elements show that this sample is relatively homogeneous in both areas, from a compositional point of view. In some locations it was observed that the deposit was not continuous, because in EDS analyzes was observed the presence of copper and zinc, specific elements of the brass substrate. Also, the presence of oxygen in elemental analysis is due to contamination of samples with water during their handling; it was visually observed that manganese oxide led to a blackish color of some zones.

The magnetic characterization of CoMnNiP coating electrodeposited in the absence of outer magnetic field was performed by vibrating sample magnetometry, plotting the hysteresis curve (fig. 4), the sample hysteresis loop being also measured after its reorientation to 90°, to estimate the magnetic anisotropy. From the allure of these two curves, can be observed that the material is isotrope and the squareness of loops is typical for ferromagnetic materials. Table 2 presents the main magnetic characteristics, determined from the hysteresis curves (fig. 4).

The magnetization data are in good agreement with the finding reported previously [47]. The values of remanence and saturation magnetization show that all CoNiMnP films are able to be magnetized and may be used rather as magnetically soft materials. The coercive force in-plane

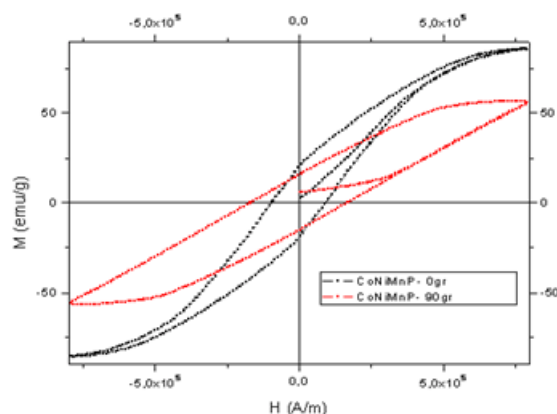


Fig. 4. The magnetic hysteresis curves of the CoMnNiP alloy deposited on brass substrate, without the external magnetic field position of the coating is 92 kA/m (1155 Oe), which is a value less than twice comparing to the coercive force in a perpendicular position.

Characterization of type 2 CoNiMnP alloys coatings (deposited on copper foil in the presence of magnetic field)

Figures 5 a - c present the morphology of the CoNiMnP alloys coating also deposited on a macro size substrate, which is in this case a copper foil of 17 cm² surface area. The SEM micrographs were made for different areas, at different magnifications, from ×2000 to ×50000. From the SEM micrographs shown in these figures it can be observed that the morphology of the coating is homogeneous and, unlike the micrographs of the CoNiMnP alloy deposited in the absence of the external magnetic field (shown in fig. 2), there have no microcracks. The surface morphology consists in crystalline grains of about 1μm in size, distributed as inflorescence aggregates.

Figures 6 show the results of EDS elemental analysis of type 2 coating. They are presented the secondary electron SEM image of CoMnNiP alloy deposited on copper foil in

State of the sample	Remanent magnetization (emu/g)	Saturation magnetization (emu/g)	Coercivity	
			(kA/m)	(Oe)
CoNiMnP film measured at 0° (in plane)	20.47	85.74	92	1155
CoNiMnP film measured at 90°	15.70	56.81	169	2125

Table 2
THE MAIN MAGNETIC FEATURES OF CoMnNiP ALLOY COATING OBTAINED BY ELECTRODEPOSITION WITHOUT EXTERNAL MAGNETIC FIELD

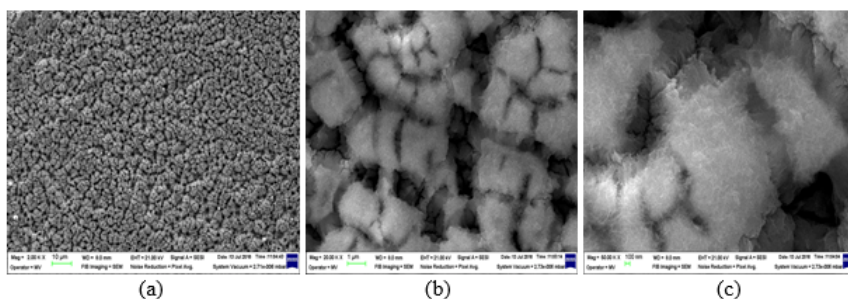


Fig. 5. Surface morphology of a type 2 CoNiMnP alloy coating exhibited by SEM images at different magnifications: ×2000 (a), ×20000 (b), and ×50000 (c)

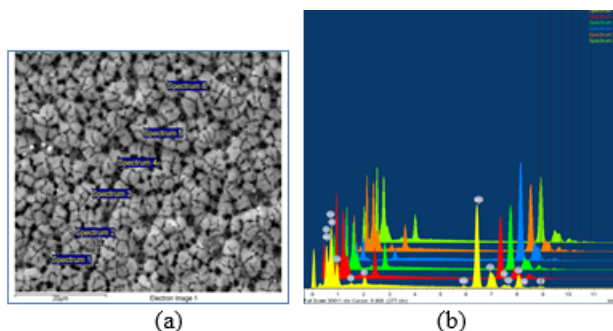


Fig. 6. Secondary electron image (a) for a type 2 CoNiMnP alloy coating electrodeposited in the presence of external magnetic field, EDS spectra (b) determined in 6 points, and relative distributions of concentration for each element (c)

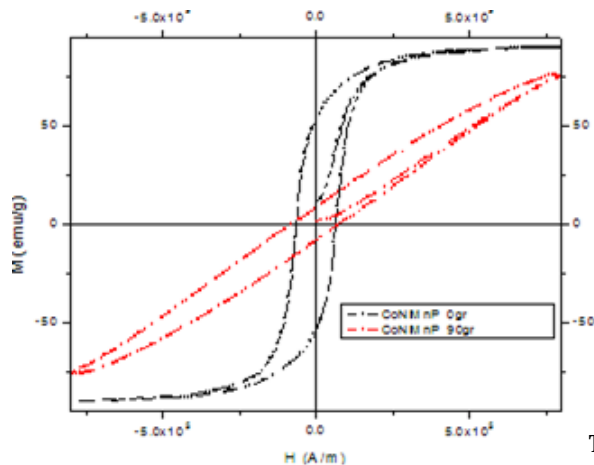


Fig. 7. The magnetic hysteresis curves of the type 2 CoMnNiP alloy deposited on copper foil substrate in the presence of the external magnetic field $H = 2T$

Table 3
THE MAIN MAGNETIC FEATURES OF TYPE 2 CoMnNiP ALLOY COATING OBTAINED BY ELECTRODEPOSITION IN EXTERNAL MAGNETIC FIELD

State of the sample	Remanent magnetization (emu/g)	Saturation magnetization (emu/g)	Coercivity	
			(kA/m)	(Oe)
CoNiMnP measured at 0° (in plane)	53.95	89.80	65	812.8
CoNiMnP measured at 90°	8.55	75.66	75.5	947.5

the presence of an external magnetic field ($H = 2T$), EDS spectra of semiquantitative composition in 6 points of a selected microarea and the distribution of the elements concentration, depending on the distance between the points. It is found that the deposited alloy had a diminished content in cobalt component (compared with films obtained without external magnets), on average approx. 50 wt.% Co, with a minimum of 18% and a maximum of 74.5%. The nickel content was between 7 and 14.8 wt.%, higher than the deposited coating without magnetic field. Manganese content is between 0 and 2 wt.%, whereas the phosphorus content is between 2.7 wt.% and 7 wt.%. However, the analyzed sample had a high oxygen content of 25 wt.%, proving the existence of metal oxides in the deposit; the content in oxygen is less for the sample with the highest cobalt concentration (74.5%). The distribution of the element concentration as well as the values of the actual concentrations of these elements show that the sample is non-homogeneous from a compositional point of view.

The magnetic characterization of a type 2 CoNiMnP alloy coating was performed by magnetometry, the sample

being measured at 0° and at 90° (see the hysteresis loops presented in fig. 7). It is noticed from the two hysteresis curves that the sample is magnetic anisotropic: the hysteresis curve at 0° is the one specific to the hard magnets, while for the 90° reorientation, the curve squareness of the magnetic material is low.

Table 3 lists the main features of the type 2 CoMnNiP magnetic layers, depending on the deposition conditions. Compared to previously analyzed samples, deposited on brass substrate without external magnetic field, there is a higher value of remanent magnetization (about 54 emu/g), but lower value of the coercive field due to the low concentration of cobalt in the electrodeposited alloy.

Characterization of types 3-5 CoNiMnP alloys coatings (deposited on brass substrate in the presence of magnetic field)

Figures 8 - 10 present the surface morphology and results of EDS analyses of the types

3 - 5 CoNiMnP alloys coatings in the presence of 2 T external magnetic field. In these cases, the films were electrodeposited on a micro size brass substrate, which had 0.24 cm² surface area for each microsample.

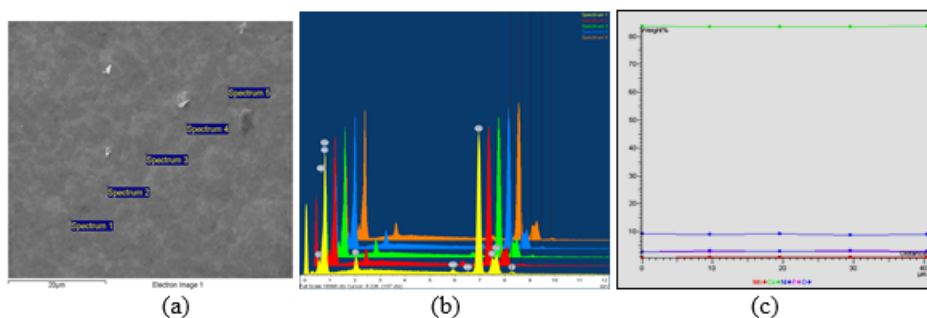


Fig. 8. Secondary electron image (a) for a type 3 CoNiMnP alloy coating electrodeposited in the presence of external magnetic field, EDS spectra (b) determined in 6 points, and relative distributions of concentration for each element (c)

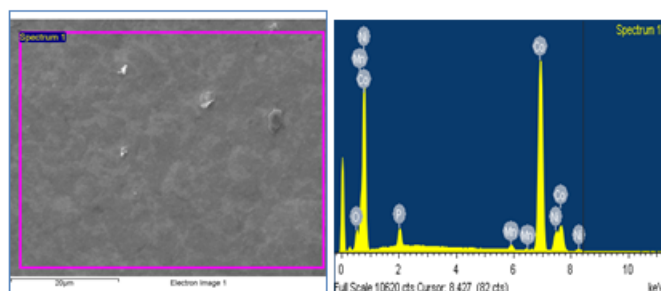


Fig. 9. Secondary electron image (a) for a type 4 CoNiMnP alloy coating electrodeposited in the presence of external magnetic field, EDS spectrum (b) determined in a single location

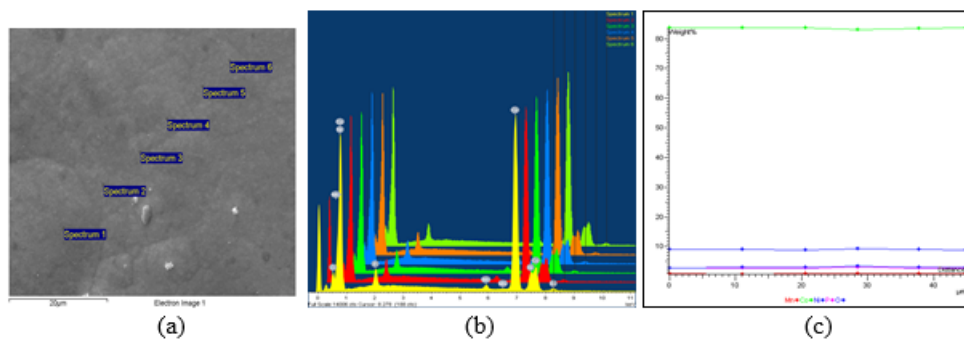


Fig. 10. Secondary electron image (a) for a type 5 CoNiMnP alloy coating electrodeposited in the presence of external magnetic field, EDS spectra (b) determined in 6 points, and relative distributions of concentration for each element (c)

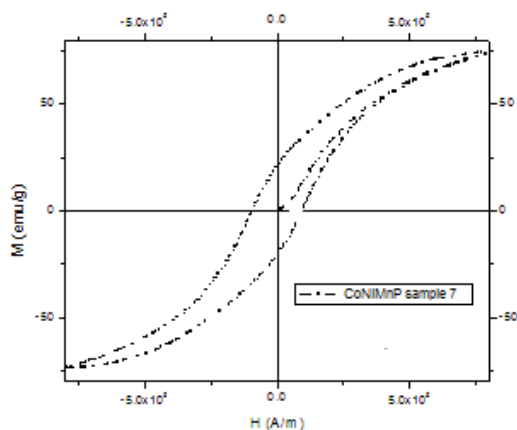


Fig. 11. The magnetic hysteresis curves of the CoMnNiP alloy deposited on brass substrate in the presence of the external magnetic field

State of the sample	Remanent magnetization (emu/g)	Saturation magnetization (emu/g)	Coercivity	
			(kA/m)	(Oe)
CoNiMnP microsample 5 (2 mA/cm ² , 24h)	19.69	73.80	88.5	1111
CoNiMnP microsample 6 (2 mA/cm ² , 24h)	20.04	71.79	91.2	1146
CoNiMnP microsample 7 (2 mA/cm ² , 24h)	20.77	73.99	95.0	1188
CoNiMnP microsample 8 (2 mA/cm ² , 24h)	15.86	64.16	92.0	1155

Table 4
THE MAIN MAGNETIC FEATURES OF TYPE 5 CoMnNiP ALLOY COATING OBTAINED BY ELECTRODEPOSITION IN EXTERNAL MAGNETIC FIELD

In the following, for the revealed microarea shown in figure 8a, the average values of the elements concentration (expressed in weight percentage) will be discussed. It is observed in figures 9b,c that the deposited alloy has high content of cobalt, on average 83.5%. Nickel content was 9.2%, manganese content was 1.0% and phosphorus was 3.0%. Interestingly, the concentration of metal oxides was low, the analyzed sample having content in oxygen averaging 3.22%. The profile of the distribution of the concentration of the highlighted elements, as well as the values of the actual concentrations of these elements show that the sample is homogeneous from the point of view of chemical composition.

Figures 9 show the SEM image for a type 4 CoNiMnP alloy coating electrodeposited in the presence of 2 T external magnetic field, as well as the EDS spectrum determined in a single point. The elemental analysis revealed that the chemical composition of CoNiMnP alloy was: 83.5% Co, 9.1% Ni, 1.0% Mn, 3.0% P and around 3.0% oxygen.

Figures 10 refer to EDS elemental analysis in 6 points of a microarea of type 5 CoNiMnP alloy. The average contents of coating were: 83.5% Co, 9.2% Ni, 1.02% Mn, 3.01% P and 3.22% oxygen. As with figures 9 and 10 (corresponding to types 3 and 4 alloys, respectively), the results confirm high cobalt concentration values for micro size samples obtained in the presence of external magnetic field as well as their homogeneity from compositional point of view.

The magnetic characterization of four different pieces (denoted as samples 5, 6, 7 and 8) belonging to type 5 CoMnNiP coating, as micro size samples, was also performed by drawing their hysteresis curves using the vibration sample magnetometer. Figure 11 shows only the magnetic hysteresis curves for 0° orientation (in plane to magnetic field) and their shape suggests a hard magnetic material. The values of the main magnetic characteristics calculated from the hysteresis curves of these samples are listed in table 4. The remanent magnetization ranged from 15.9 to 20.8 emu/g, saturation magnetization was in the range 64 - 74 emu/g, and coercivity was in the 1111 - 1188 Oe range.

Conclusions

CoNiMnP permanent magnetic alloys were successfully electrodeposited on copper and brass substrates from a bath containing CoCl₂, NiCl₂, MnSO₄, NaH₂PO₄, as precursors and H₃BO₃, NaCl, saccharin, sodium lauryl sulphate and cerium(III) sulphate as additives. In the absence of magnetic field some microcracks are present on their surface that proves the presence of stress forces inside the grown deposit. The coatings obtained using external magnetic field (of 2 T) on macro size (17 cm²) copper substrate were continuous, homogeneous, smooth, and have a bright gray color. The SEM images showed an insular-type morphology containing fine spherical nodules evenly spread, whose composition is rich in cobalt according to

EDS elemental analysis. Grain crystals of about 1 μm in size are distributed as inflorescence aggregates.

The magnetic characterization of CoNiMnP macro size coatings by their hysteresis loops at different angles, 0° and 90° , indicates a magnetic isotropy and a shape of loops that is typical for ferromagnetic materials with rather soft magnetism. In the absence of external field during electrodeposition the coercive force in-plane position of the coating is less than twice comparing to the coercive force in a perpendicular position. However, in the presence of a 2 T magnetic field both values of coercivity are similar.

The CoNiMnP coatings electrodeposited on micro size brass substrate were homogeneous from compositional point of view, with the average content (in weight percentage) of 83.5% Co, 9.2% Ni, 1.0% Mn, 3.0% P and 3.2% oxygen. The shape of their magnetic hysteresis curves for 0° orientation suggests a hard magnetic material. Regarding the magnetic characteristics calculated from the hysteresis curves, values of remanent magnetization ranged from 15.9 to 20.8 emu/g, saturation magnetization was in the range 64 - 74 emu/g, and coercivity was in the 1111 - 1188 Oe range.

Acknowledgement: Financial support is gratefully acknowledged from the Executive Agency for Higher Education, Research Development & Innovation Funding: 2nd R&DI National Programme: Electromagnetic and electrodynamic actuators manufactured through LIGA technology" (ctr. PN II No. 249 / 2014).

References

- DATTA, M., LANDOLT, D., Fundamental aspects and applications of electrochemical microfabrication, *Electrochim. Acta*, **45**, 2000, p. 2535-2358.
- SUTANTO, J., LUHARUKA, R., HESKETH, P. J., BERTHELOT, Y. H., Designing and fabricating electromagnetically actuated microvalves for MEMS applications, *Sensors Mater.*, **19**, no. 1, 2007, p. 35-56.
- HERRERA - MAY, L. A., AGUILERA - CORTÉS, L. A., GARCÍA - RAMIREZ, P. J., MANJARREZ, E., Resonant magnetic field sensors based on MEMS technology, *Sensors*, **9**, 2009, p. 7785-7813.
- TODARO, M. T., SILEO, L., VITTORIO, DE. M., Magnetic field sensors based on microelectromechanical systems (MEMS) technology, chapter 6 in: *Magnetic Sensors. Principles and Applications*, K. Kuang (Ed.), InTeCh, Rijeka, Croatia, 2012.
- SCHIAVONE, G., DESMULLIEZ, M. P. Y., WALTON, A. J., Integrated magnetic MEMS relays: Status of the technology, *Micromachines*, **5**, 2014, p. 622-653.
- NIARCHOS, D., Magnetic MEMS: Key Issues and Some Applications, *Sensors and actuat.*, **A**, **106**, 2003, p. 255-62.
- SPELIOTIS, TH., NIARCHOS, D., Deposition of hard magnetic SmCo₅ thin films by magnetron sputtering, *J. of Phys.: Conf. Series*, **10**, 2005, p.175.
- PATROI, D., CODESCU, M. M., PATROI, E. A., MARINESCU, V., Structural and magnetic behaviour of DC sputtered Alnico type thin films, *Optoel. and Adv. Mater. -Rapid Comm.*, **5**, no. 10, 2011, p. 1130 -1133.
- CONSTANTINESCU, C., ION, V., CODESCU, M. M., ROTARU, P., DINESCU, M., Optical, morphological and thermal behavior of NdFeB magnetic thin films grown by radiofrequency plasma-assisted pulsed laser deposition, *Curr. Appl. Phys.*, **13**, no. 9, 2013, p. 2019 - 2025.
- CONSTANTINESCU, C., PATROI, E. A., CODESCU, M. M., DINESCU, M., Effect of nitrogen environment on NdFeB thin films grown by radio frequency plasma beam assisted pulsed laser deposition, *Mater. Sci. and Engin. B*, **178**, 2013, p. 267 - 271.
- YOSHINARI, J., MORITA, H., TOKUOKA, Y., Fe-C-O amorphous thin film by plasma CVD, *IEEE Trans. on Magn.*, **21**, no. 5, 1985, p. 2047 - 2049.
- HOMMA, T., KITA, Y., OSAKA, T., Electrochemical Studies on the Deposition Process of Electroless CoNiP Films with Graded Magnetic Properties, *J. of Electrochem. Soc.*, **147**, no. 11, 2000, p. 4138 - 4141.
- PATTANAIAK, G., KIRKWOOD, D. M., XU, X., ZANGARI, G., Electrodeposition of hard magnetic films and microstructures, *Electrochim. Acta*, **52**, no. 8, 2007, p. 2755 - 2764.
- HORKANS, J., SEAGLE, D. J., CHANG, I. H., Electroplated magnetic media with vertical anisotropy, *J. Electrochem. Soc.*, **137**, no. 7, 1990, p. 2056-2061.
- CHIN, T., Permanent magnet films for applications in micromechanical systems, *J. Magn. Magn. Mater.*, **209**, 2000, p. 75-79.
- BHALIS, DE. D., MURRAY, C., DUFFY, M., ALDERMAN, J., KELLY, G., MATHUNA, S. C. O., Modeling and analysis of a magnetic microactuator, *Sensors Actuat.*, **81**, 2000, p. 285-289.
- SETNESCU, R., SETNESCU, T., JIPA, S., KAPPEL, W., DUMITRU, M., CODESCU, M. M., STANCU, N., ZAHARESCU, T., Magnetic Flexible Material containing Microcrystalline NdFeB Powder, *J. of Optoel. and Adv. Mater.*, **8**, no. 2, 2006, p. 533 - 537.
- PRIOTEASA, P., ILIE, C., POPA, M., IORDOC, M., SBARCEA B. G., Electrodeposition of nickel for fabrication of microfluidic pumps, *Rev. Chim. (Bucharest)*, **64**, no. 3, 2013, 275-280.
- LIU, C., Development of surface micromachined magnetic actuators using electroplated permalloy, *Mechatronics*, **8**, 1998, p. 613-633.
- LIU, C., TSAO, T., Lee, G., LEU, J. T. S., YI, Y. W., TAI, Y. C., HO, C., Out of plane permalloy magnetic actuators with electroplated permalloy for fluid dynamics control, *Sensors Actuat.*, **78**, 1999, p. 190-197.
- MYUNG, N. V., PARK, D. YOO, B. Y., SUMODJO, P. T. A., Development of electroplated magnetic materials for MEMS, *J. Magnetism Magnetic Mater.*, **265**, 2003, p. 189-198.
- CHOU, M. C., YANG, H., YEH, S. H., Microcomposite electroforming for LIGA technology, *Microsyst. Technol.*, **7**, 2001, p. 36-39.
- GOLODNITSKY, D., ROSENBERG, Y., ULUS, A., Role of anion additives in the electrodeposition of Ni-Co alloy from sulfamate electrolyte, *Electrochim. Acta*, **47**, 2002, p. 2707-2714.
- KIM, D., PARK, D. Y., B. Y. YOO, P. T. A. SUMODJO, P. T. A., MYUNG, N. V., Magnetic properties of nanocrystalline iron group thin film alloys electrodeposited from sulfate and chloride baths, *Electrochim. Acta*, **48**, 2003, p. 819-830.
- YOO, B. Y., HERNANDEZ, S. C., PARK, D. Y., MYUNG, N. V., Electrodeposition of FeCoNi thin films for magnetic-MEMS devices, *Electrochim. Acta*, **51**, 2006, p. 6346-6352.
- CHUNG, C. K., CHANG, W. T., Effect of pulse frequency and current density on anomalous composition and nanomechanical property of electrodeposited Ni-Co films, *Thin Solid Films*, **617**, no. 17, 2009, p. 4800-4804.
- QIN, L., LIAN, J., JIANG, Q., Enhanced ductility of high-strength electrodeposited nanocrystalline Ni-Co alloy with fine grain size. *J. Alloys Compd.*, **504**, no. 1, 2010, p. 439-442.
- COJOCARU, P., MAGAGNIN, L., GOMEZ, E., VALLES, E., Electrodeposition of CoNi and CoP alloys in sulphamate electrolytes, *J. Alloys Compd.*, **503**, 2010, p. 454-459.
- P. SUDHAKAR, B.S.S. DANIEL, P. JEEVANANDAM, Synthesis of nanocrystalline Co-Ni alloys by precursor approach and studies on their magnetic properties, *J. Magn. Magn. Mater.*, **323**, no. 17, 2011, p. 2271-2280.
- ARENAS, J. V., TREERATANAPHITAK, T., PRITZKER, M., Formation of Co-Ni alloy coatings under direct current, pulse current and pulse-reverse plating conditions, *Electrochim. Acta*, **62**, no. 15, 2012, p. 63-72.
- KIM, D., AOKI, K., TAKANO, O., Soft magnetic films by electroless Ni-Co-P plating, *J. Electrochem. Soc.*, **142**, no. 11, 1995, p. 3763-3767.
- MATSUBARA, H., YAMADA, A., Control of magnetic properties of chemically deposited cobalt nickel phosphorus films by electrolysis, *J. Electrochem. Soc.*, **141**, no. 9, 1994, p. 2386-2390.

33. GUAN, S., NELSON, B. J., Pulse-reverse electrodeposited nanograin-sized CoNiP thin films and microarrays for MEMS actuators, *J. Electrochem. Soc.*, **152**, no. 4, 2005, p. C190-C195.
34. LI, D., WU, C., WANG, Q., CHOPART, J. P., HE, J., FRANCAZAK, A., LEVESQUE, A., Effects of high magnetic field postannealing on microstructure and properties of pulse electrodeposited Co-Ni-P films, *Adv. Mater. Sci. Eng.*, 2016, Article ID 3816972, 6 pages.
35. VIEUX-ROCHAZ, L., DIEPPEDALE, C., DESLOGES, B., GAMET, D., BARRAGATTI, C., ROSTAING, H., MEUNIER-CARUS, J., Electrodeposition of hard magnetic CoPtP material and integration into magnetic MEMS, *J. Micromech. Microeng.*, **16**, no. 2, 2006, p.219-224.
36. M. KRISHNAPPA, M. R., RAJASEKARAN, N., GANESAN, S., EMERSON, R. N., Mechanical and magnetic properties of electrodeposited CoMnP thin film alloys, *J. Eng. Appl. Sci.*, **6**, no. 1, 2011, p. 21-26.
37. LIAKOPOULOS, T. M., ZHANG, W., AHN, C. H., Electroplated thick CoNiMnP permanent magnet arrays for micromachined magnetic device applications, *Proc. 1996 IEEE MEMS Conf.*, San Diego, 1996, p. 79-84.
38. CHO, H. J., BHANSALI, S., AHN, C. H., Electroplated thick permanent magnet arrays with controlled direction of magnetization for MEMS application, *J. Appl. Phys.*, **87**, no. 9, 2000, p. 6340-6342.
39. CHO, H. J., AHN, C.H., A bidirectional magnetic microactuator using electroplated permanent magnet arrays, *J. Microelectromech. Syst.*, **11**, no. 1, 2002, p. 78-84.
40. GUAN, S., NELSON, B. J., Electrodeposition of low residual stress CoNiMnP hard magnetic thin films for magnetic MEMS actuators, *J. Magn. Magn. Mater.*, **292**, 2005, p.49-58.
41. GRAPES, M. D., MORRIS, C. J., Optimizing the CoNiMnP electrodeposition process using Taguchi design of experiments, *J. Electrochem. Soc.*, **157**, no. 12, 2010, p. D642-D647.
42. MORRIS, C. J., ISAACSON, B., GRAPES, M. D., DUBEY, M., Self-assembly of microscale parts through magnetic and capillary interactions, *Micromachines*, **2**, 2011, p. 69-81.
43. SUN, X. M., YUAN, Q., FANG, D. M., ZHANG, H. X., Electrodeposition and characterization of CoNiMnP-based permanent magnetic film for MEMS applications, *Proc. of the 6th IEEE Int. Conf. on Nano/Micro Engineered and Molecular Systems*, Febr. 20-23, 2011, Kaohsiung, Taiwan.
44. SUN, X., YUAN, Q., FANG, D., ZHANG, H., Electrodeposition and characterization of CoNiMnP permanent magnet arrays for MEMS sensors and actuators, *Sens. Actuat. A: Physical*, **188**, 2012, p. 190-197.
45. QU, N. S., JIAO, F., Fabrication of CoNiMnP-BaFe₁₂O₁₉ nanocomposite coatings by electrodeposition, *Trans. IME*, **90**, no. 2, 2012, p. 92-97.
46. QU, N.S., JIAO, F., Improvement of magnetic properties of electrodeposited CoNiMnP-BaFe₁₂O₁₉ nanocomposite coatings in presence of sodium lauryl sulphate, *Trans. IME*, **91**, no. 2, 2013, p. 88-95.
47. PRIOTEASA, P., CODESCU, M. M., PATROI, E. A., PATROI, D., MARINESCU, V., Electroplating in magnetic field and characterization of NiCoMnP alloy films with permanent magnet, *Optoelectr. Adv. Mater. Rapid Commun.*, **7**, no. 1-2, 2013, p. 90-95.

Manuscript received: 1.08.2017